Spin and orbital magnetism of a single 3*d* transition-metal atom doped into icosahedral coinage-metal clusters X_{12} (X = Cu, Ag, Au)

Mahdi Sargolzaei[1,2,*] and Neda Lotfizadeh[1]

[1]*Department of Physics, Iran University of Science and Technology, Narmak 16345, Tehran, Iran*

[2]*Computational Physical Science Laboratory, Department of Nano-Science, Institute for Research in Fundamental Sciences (IPM), Tehran, Iran*

(Received 20 December 2010; published 4 April 2011)

We have demonstrated the electronic structures and magnetic properties of single 3*d* transition metal (TM) atoms encapsulated in noble metal clusters with icosahedral symmetry in the framework of relativistic density functional theory. Orbital polarization corrections have been used to obtain an upper-estimation for orbital magnetic moments of all individual 3*d* atoms. The relativistic corrections are marginally affected the spin magnetic moments, whereas they induce significant orbital magnetism in TM@X_{12} icosahedra. It is found that a *superatomic* picture has to be taken into account in order to explain the spin and orbital magnetism induced in TM@X_{12} icosahedron based on the Hund's rules.

DOI: 10.1103/PhysRevB.83.155404 PACS number(s): 75.30.Hx, 75.70.Tj, 75.75.Lf, 61.46.−w

I. INTRODUCTION

Intriguing possibility of magnetism and structural properties of noble metal clusters and their compositions have triggered great research interests due to their potential applications in cell- and virus-active nanoparticles, molecular electronics, and building blocks for spin functional nanodevices.[1–4] Despite a great challenge for synthesis and stabilization of a desired noble metal cluster,[5–9] many theoretical,[10–18] and experimental[19–24] studies have been devoted to the electronic and structural properties of coinage metal clusters. A promising class of structures are neutral icosahedra with I_h symmetry known as magic clusters[1,25] in which one TM atom coordinated at the center of the X_{12} icosahedron formed by peripheral noble atoms. In spite of the fact that an icosahedral symmetry is not necessarily the ground state for all TM@X_{12} clusters,[16,26] however an icosahedron is an interesting object due to its unique symmetry operations (apart from spherical symmetry, the icosahedron has highest symmetry possible for a three-dimensional object) and may act as a large atomic-like packing unit. Therefore depending on its electronic configurations it may show large local magnetism. It has also been found that doping one TM atom into the center of the object may stabilize the noble metal icosahedra.[27–32] Sun and co-workers in their density functional theory level have found that the TM@Cu_{12} and TM@Ag_{12} icosahedra are relatively more stable than the Cu@Cu_{12} (≡Cu_{13}) and Ag@Ag_{12} (≡Ag_{13}) icosahedral clusters.[33,34] The heavier homologs TM@Au_{12} are found to be more stable than the Au@Au_{12} (≡Au_{13}) icosahedron.[35] Pyykko and Runeberg have predicted that the W@Au_{12} icosahedron is also stable[27] which is later confirmed experimentally by Li and co-workers.[28]

On the other hand, a single TM atom encapsulated in a noble metal host is a promising candidate to show how spin and orbital magnetism can be formed around a single impurity due to the interaction of its valence electrons with nearly free electrons of the peripheral noble metal atoms.[36–39] It should be noted that more degrees of freedom in a molecule or a prototype cluster compared to bulk phase induce a tendency for orbital ordering and hence provide opportunities to observe a sizable electronic orbital angular momentum and intricate interplay between the spin and orbital magnetic moments, which is pronounced for a significant spin-orbit (SO) interaction. The SO coupling in its average form (SR = scalar relativistic) or exact form (FR = full relativistic) is known to be extremely important to give a reliable electronic structure particularly for heavy fermionic systems such as gold.[40–42] In addition, the exact form of SO interaction has to be taken into account for an adequate description of certain aspects of magnetism like the magneto-optical effect, magnetic anisotropy energy, and orbital magnetism.[43] The SR and nonrelativistic approaches have been widely used to consider the spin magnetism in noble metal clusters and their compositions.[44–47] Wang and co-workers using a state-of-the-art SR real-space first-principles cluster method have found that binary three-dimensional icosahedra (TM@Au_{12}) with integer total magnetic moments can be stabilized.[35] This finding was pronounced for a superatomic perspective in TM@Au_{12} icosahedra. The same scenarios have been found for TM@Cu_{12} and TM@Ag_{12} clusters by Sun and co-workers based on spin density functional theory calculations in a nonrelativistic regime.[33,34] However, Sun and co-workers have also argued that in Sc@Ag_{12} and Ni@Ag_{12} clusters the deviation of electronic configuration from the superatomic picture is relatively large. The calculated total magnetic moments of Sc@Ag_{12} and Ni@Ag_{12} were found to be 1.77 μ_B and 2.31 μ_B, respectively. They have also reported a very small total of magnetic moments of 0.36 μ_B for Cu_{13} and 0.28 μ_B for Ag_{13} icosahedral clusters.[33,34] For those TM@X_{12} clusters that follow the superatomic picture a quintuply degenerate h_g molecular orbital (MO) as highest occupied molecular orbitals (HOMO) can merely explain the induced integer numeral regime for spin magnetism. These HOMO levels of TM@X_{12} are formed mostly from the valence d states of TM atoms and valence *spd* orbitals of noble metal atoms. It has to be pointed out that in SR or nonrelativistic calculations the related h_g HOMO's remain quintuply degenerate. However, in the FR regime, the degeneracy of the h_g molecular orbitals will be reduced which also split the valence *d* states of TM atoms in h_g molecular orbitals. This is subject to enhanced orbital

ordering in the valence d electrons of the central TM atom in TM@X_{12} icosahedra.

The purpose of the present work is to study the advantages and disadvantages of spin and orbital magnetism in TM@X_{12} with icosahedral structure. To the best of our knowledge the SO interaction has not yet been taken into account to study the orbital magnetism induced in a 13-atom icosahedron formed by noble and 3d transition metals. Here, the hitherto unanswered question is that Hund's rules are still valid in an icosahedron or not. In this study, we will demonstrate that in order to preserve Hund's second rule, a superatomic picture instead of a single atomic picture has to be taken into account to explain the induced orbital magnetism in an icosahedron. The paper is organized as follows. Section II contains details about the cluster structure and the numerics. Section III presents the results and discussion (structural properties and calculated spin and orbital magnetic moments). Finally, the paper is summarized in Sec. IV.

II. COMPUTATIONAL METHOD

Our density functional calculations[48] on the electronic structures and magnetic properties of TM@X_{12} noble metal clusters based upon the relativistic version[43] of the all-electron full-potential local-orbital method using the FPLO-9 package.[49] In this scheme, the full relativistic calculations have been performed self-consistently on the four-component Kohn-Sham-Dirac (KSD) equation, which implicitly contains spin-orbit coupling up to all orders. The scalar relativistic approach has also been implemented within a spherically average on the spin-orbit interaction. The Perdew-Burke-Ernzerhof 96 of the generalized gradient approximation (GGA) was used for the exchange-correlation (XC) potential.[50] In the molecular mode of the FPLO package, a single 3d TM atom has been added to the center of the icosahedron under I_h symmetry formed by noble metals (see Fig. 1). The valence basis set was comprised of 3d TM (3s, 3p, 3d, 4s, 4p, 4d, 5s), silver (4s, 4p, 4d, 5s, 5p, 5d, 6s), gold (5s, 5p, 5d, 6s, 6p, 6d, 7s) states. The site-centered potentials and densities were expanded in spherical harmonic contributions up to $l_{\max} = 12$. For a self-consistent field iteration, the charge density is converged to 1×10^{-6}, and a total energy convergence of 0.001 meV. In structural optimization, the atoms are relaxed until the force on each atom was less than 0.001 eV/Å. Resulting GGA orbital magnetic moments of 3d transition metals were expected as a lower estimate, and to get an upper estimate of orbital magnetism we used an OP correction suggested by Eriksson and co-workers[51] and extended by Eschrig and co-workers[52,53] in a spin dependent form for incompletely filled d shells. In analogy to the Stoner theory for spin magnetism,[54] the OP correction functional which is proportional to squared total orbital momentum, was added to the GGA functional. The binding energy (E_b) for a neutral cluster is determined as $E_b = E_a - E_t$, where E_a is the sum of the total energies of all single atoms and E_t is the total energy of the relaxed cluster.

In order to check the validity of the current computational scheme, we first performed calculations on the Cu_2, Ag_2, and Au_2 dimers. The obtained bond lengths and binding energies of these dimers are as follows: (2.23 Å, 2.22 eV) for Cu_2, (2.58 Å, 1.71 eV) for Ag_2, and (2.53 Å, 2.24 eV) for Au_2 dimers. One can compare our results to those of experimental values for Cu_2 (2.22 Å, 2.05 eV),[7] Ag_2 (2.48 Å, 1.65 eV),[55] and Au_2 (2.47 Å, 2.29 eV)[56] dimers, respectively. These excellent agreements between the calculated and experimental data suggest the reliability of the theoretical method employed in the present work.

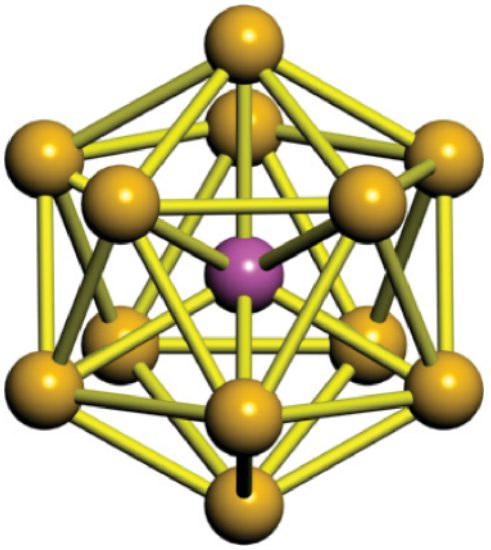

FIG. 1. (Color online) Icosahedral noble metal cage doped with one 3d atom (TM@X_{12}); the center ball represents 3d TM atom and the peripheral spheres indicate the noble metal atoms (X = Cu, Ag, and Au).

III. RESULTS AND DISCUSSION

As a starting point of discussion first we study the electronic properties of HOMO levels in the TM@X_{12} icosahedra. Figure 2 shows the HOMO levels of TM@Au_{12} clusters for TM series from Sc to Cu. They have Lorentzian shapes with a width of 0.1 eV. Using integration over a whole range of energies we have shown that the degeneracy of HOMO levels in TM@Au_{12} is equal to 5, which guarantees h_g symmetry in the HOMO levels. The same symmetry was found for the HOMO levels of TM@Cu_{12} and TM@Ag_{12} clusters. Within

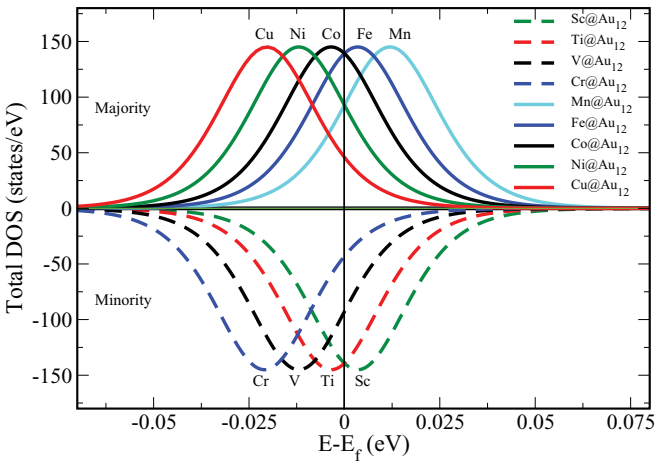

FIG. 2. (Color online) The spin-dependent HOMO levels for icosahedral TM@Au_{12}. The solid vertical line shows the Fermi level.

TABLE I. The calculated binding energies E_b (in eV), and average bond lengths between central TM and peripheral noble metal atoms R (Å) in the framework of the scalar-relativistic approach. The HOMO and LUMO and one level below the HOMO level (B-HOMO) states including symmetry and spin are given. The n_h's are the electron occupation numbers in the corresponding HOMO levels. The HOMO-LUMO gaps ΔE (in eV) are presented.

TM	n_h	E_b (R)	B-HOMO	HOMO	LUMO	ΔE
Cu_{12}:						
Sc	2	30.73 (2.50)	$h_g(+)$	$h_g(-)$	$a_g(+)$	1.72
Ti	3	33.17 (2.46)	$h_g(+)$	$h_g(-)$	$a_g(+)$	1.69
V	4	32.89 (2.43)	$h_g(+)$	$h_g(-)$	$a_g(+)$	1.65
Cr	5	31.10 (2.41)	$t_{2g}(\pm)$	$h_g(\pm)$	$a_g(\pm)$	1.51
Mn	1	30.13 (2.40)	$h_g(-)$	$h_g(+)$	$a_g(+)$	0.65
Fe	2	31.11 (2.40)	$h_g(-)$	$h_g(+)$	$h_g(-)$	0.68
Co	3	31.12 (2.40)	$h_g(-)$	$h_g(+)$	$h_g(-)$	0.52
Ni	4	30.29 (2.41)	$h_g(-)$	$h_g(+)$	$h_g(-)$	0.43
Cu	5	28.36 (2.42)	$t_{2g}(-)$	$h_g(+)$	$h_g(-)$	0.45
Ag_{12}:						
Sc	2	23.41 (2.80)	$h_g(+)$	$h_g(-)$	$a_g(+)$	1.64
Ti	3	24.74 (2.77)	$h_g(+)$	$h_g(-)$	$a_g(+)$	1.65
V	4	23.98 (2.74)	$h_g(+)$	$h_g(-)$	$h_g(+)$	1.27
Cr	5	22.28 (2.73)	$h_g(+)$	$h_g(-)$	$h_g(+)$	1.02
Mn	1	21.76 (2.72)	$h_g(-)$	$h_g(+)$	$a_g(+)$	0.72
Fe	2	22.78 (2.72)	$h_g(-)$	$h_g(+)$	$h_g(-)$	0.65
Co	3	22.90 (2.72)	$h_g(-)$	$h_g(+)$	$h_g(-)$	0.43
Ni	4	22.29 (2.72)	$h_g(-)$	$h_g(+)$	$h_g(-)$	0.37
Cu	5	20.62 (2.73)	$t_{2g}(-)$	$h_g(+)$	$h_g(-)$	0.40
Ag	5	19.36 (2.80)	$t_{2g}(-)$	$h_g(+)$	$h_g(-)$	0.41
Au_{12}:						
Sc	2	31.52 (2.77)	$h_g(+)$	$h_g(-)$	$t_{2g}(+)$	2.22
Ti	3	32.62 (2.74)	$h_g(+)$	$h_g(-)$	$h_g(+)$	1.76
V	4	31.29 (2.73)	$h_g(+)$	$h_g(-)$	$h_g(+)$	1.16
Cr	5	28.97 (2.71)	$h_g(+)$	$h_g(-)$	$h_g(+)$	0.76
Mn	1	28.53 (2.71)	$h_g(-)$	$h_g(+)$	$h_g(-)$	1.34
Fe	2	29.52 (2.71)	$h_g(-)$	$h_g(+)$	$h_g(-)$	0.74
Co	3	29.40 (2.71)	$h_g(-)$	$h_g(+)$	$h_g(-)$	0.46
Ni	4	28.84 (2.71)	$h_g(-)$	$h_g(+)$	$h_g(-)$	0.32
Cu	5	27.22 (2.72)	$t_{2g}(-)$	$h_g(+)$	$h_g(-)$	0.34
Au	5	25.53 (2.79)	$t_{2g}(-)$	$h_g(+)$	$h_g(-)$	0.35

the same method of integration in the range of $\{-\infty, \varepsilon_F\}$ we calculated the electron occupation number in the HOMO levels (n_h) and results are listed in Table I. The components of HOMO levels for two example clusters Co@Au_{12} and Au_{13} are shown in Fig. 3. It can be seen that mostly the 6*s* states and partially the 5*d* and 6*p* states of peripheral Au atoms make the HOMO levels in Au-based clusters. The 3*d* (4*d*) states of Co in Co@Au_{12} and 5*d* (6*d*) states of central Au in Au_{13} have small (very small) contributions to the HOMO level. All other states do not have contribution in the HOMO level. The same trends were found for the components of corresponding HOMO levels in TM@Cu_{12} and TM@Ag_{12} icosahedral clusters. It has to be pointed out that although the contribution of 3*d* states of TM atoms is rather weak in the HOMO level however they play an important role to figure out orbital magnetism in the TM@X_{12} icosahedra. This point will be discussed later. The calculated binding energies E_b in the SR approach and average bond lengths between central TM and peripheral noble metal atoms,

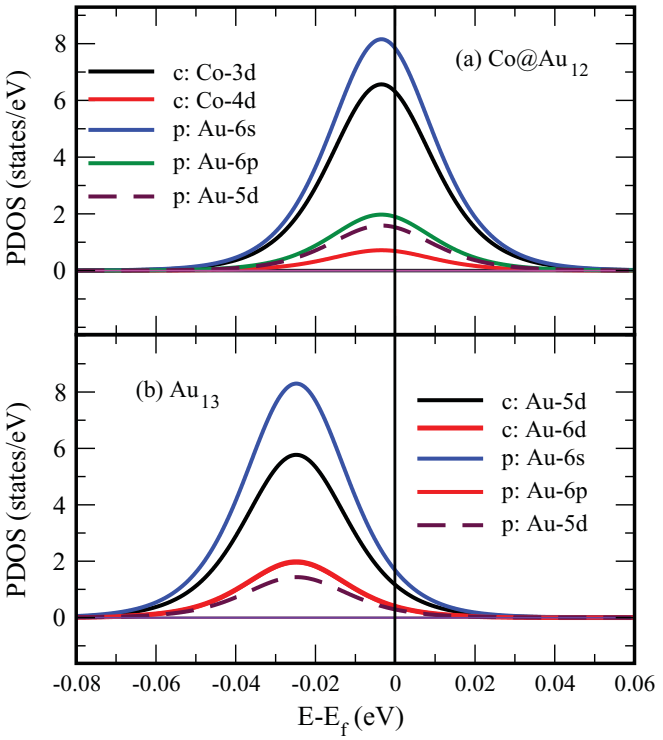

FIG. 3. (Color online) The resolved partial densities of states as components of the HOMO levels in (a) Co@Au_{12} and (b) Au_{13} icosahedra. The c: (p:) denotes for the central (peripheral) atom. The HOMO levels are formed with the combination of components: 12(p:Au) + 1(c:Co) in Co@Au_{12} and 12(p:Au) + 1(c:Au) in Au_{13}.

for all mentioned TM@X_{12} clusters are listed in Table I. Our calculated binding energies show that all the doped TM@X_{12} clusters have larger binding energies than those of the pure X_{13} clusters with I_h symmetry. Therefore one can conclude that the doped clusters have more relative stability compared to the bare X_{13} icosahedron. In the case of Cu-based clusters, doping 3*d* atoms in the Cu_{12} icosahedron opens an energy gain up to 4.8 eV compared to the Cu_{13} icosahedron. For silver- and gold-based clusters the energy gains are up to 5.4 eV and 7.1 eV, respectively (see Table I). These relative stabilities can be merely explained according to the simple fact that the 5*d* states of the central Au atom in the case of Au_{13} are almost occupied and the 6*s*-5*d* hybridization is rather weak compared to the 6*s*-3*d* hybridization in TM@Au_{12} clusters which leads to a smaller binding energy for Au_{13} cluster. The 4*s*4*p* and 6*s*6*p* of central atoms, either TM atoms or central gold atoms, have weakly interacted to the valence states of the peripheral gold atoms. Here we study the Au-based clusters, however the above reasons can be readily extended to the Cu- and Ag-based clusters which are also studied by Sun and co-workers.[33,34] We also provided the energy gaps between the HOMO and the lowest unoccupied molecular orbitals (LUMO) of the mentioned icosahedra which is another useful quantity to explain the relative stability of the TM@X_{12} icosahedra. In Table I it can be seen that those TM@X_{12} clusters with light 3*d* TM atoms have the larger HOMO-LUMO gaps than the heavier 3*d* TM atoms while the former may have high chemical inertness compare to the TM@X_{12} clusters with heavier 3*d* TM atoms. Therefore, it can be argued that the

TABLE II. The calculated local spin (M_s^{3d}) and orbital magnetic moments (M_l^{3d}) of $3d$ atoms, local spin magnetic moment of noble metal atoms (M_s^X, X = Cu, Ag, Au), and total magnetic moments ($M_T = M_s^{3d} + M_l^{3d} + 12M_s^X$) of the clusters, in scalar and fully relativistic approaches, and with orbital polarization (OP) correction. All values are in Bohr magnetons (μ_B).

	TM@Cu_{12}			TM@Ag_{12}			TM@Au_{12}		
TM/method	M_s^{3d} (M_l^{3d})	M_s^{Cu}	M_T	M_s^{3d} (M_l^{3d})	M_s^{Ag}	M_T	M_s^{3d} (M_l^{3d})	M_s^{Au}	M_T
Sc (SR)	0.142 (0.000)	0.238	3.000	0.430 (0.000)	0.214	3.000	0.126 (0.000)	0.240	3.000
FR	0.140 (0.002)	0.237	2.989	0.430 (0.066)	0.214	3.059	0.121 (0.155)	0.194	2.600
FR + OP	0.139 (0.001)	0.238	2.987	0.431 (0.079)	0.213	3.072	0.121 (0.163)	0.193	2.605
Ti (SR)	0.203 (0.000)	0.150	2.000	0.758 (0.000)	0.104	2.000	0.299 (0.000)	0.142	2.000
FR	0.196 (−0.042)	0.149	1.942	0.751 (0.033)	0.104	2.028	0.300 (0.276)	0.114	1.939
FR + OP	0.191 (−0.085)	0.149	1.899	0.744 (−0.017)	0.104	1.978	0.310 (0.333)	0.112	1.992
V (SR)	0.237 (0.000)	0.064	1.000	1.515 (0.000)	−0.043	1.000	0.982 (0.000)	0.001	1.000
FR	0.220 (−0.070)	0.062	0.894	1.523(0.071)	−0.043	1.071	0.908 (0.192)	0.005	1.166
FR + OP	0.211 (−0.137)	0.063	0.828	1.526(0.136)	−0.044	1.136	0.905 (0.297)	0.005	1.266
Cr (SR)	0.000 (0.000)	0.000	0.000	2.867 (0.000)	−0.239	0.000	2.774 (0.000)	−0.231	0.000
FR	0.000 (0.000)	0.000	0.000	2.871 (−0.039)	−0.239	−0.031	2.795 (−0.007)	−0.205	0.323
FR + OP	0.000 (0.000)	0.000	0.000	2.871 (−0.046)	−0.238	−0.038	2.783 (0.046)	−0.205	0.372
Mn (SR)	2.174 (0.000)	−0.098	1.000	3.484(0.000)	−0.207	1.000	3.772 (0.000)	−0.231	1.000
FR	2.165 (−0.380)	−0.097	0.617	3.477 (−0.237)	−0.206	0.765	3.797 (−0.354)	−0.202	1.019
FR + OP	2.089 (−0.607)	−0.091	0.390	3.466 (−0.280)	−0.205	0.722	3.786 (−0.400)	−0.201	0.975
Fe (SR)	2.327 (0.000)	−0.027	2.000	2.806 (0.000)	−0.067	2.000	3.208(0.000)	−0.101	2.000
FR	2.304 (−0.383)	−0.026	1.606	2.782 (−0.258)	−0.067	1.716	3.195 (−0.467)	−0.093	1.615
FR + OP	2.225 (−0.523)	−0.020	1.465	2.763 (−0.295)	−0.066	1.679	3.183 (−0.644)	−0.090	1.455
Co (SR)	1.582 (0.000)	0.118	3.000	1.719 (0.000)	0.107	3.000	2.069 (0.000)	0.078	3.000
FR	1.549 (−0.307)	0.118	2.658	1.688 (−0.095)	0.103	2.828	1.999 (−0.348)	0.042	2.157
FR + OP	1.487 (−0.387)	0.123	2.577	1.677 (−0.062)	0.104	2.859	1.996 (−0.655)	0.046	1.893
Ni (SR)	0.807 (0.000)	0.266	4.000	0.757 (0.000)	0.270	4.000	0.985 (0.000)	0.251	4.000
FR	0.783 (−0.135)	0.263	3.805	0.707 (−0.120)	0.258	3.684	0.367 (0.047)	0.047	0.983
FR + OP	0.769 (−0.147)	0.264	3.791	0.690 (−0.113)	0.259	3.679	0.000 (0.000)	0.000	0.000
Cu (SR)	0.242 (0.000)	0.396	5.000	0.157 (0.000)	0.403	5.000	0.236(0.000)	0.397	5.000
FR	0.239 (0.028)	0.392	4.986	0.151 (0.028)	0.394	4.909	0.108(0.091)	0.186	2.437
FR + OP	0.239 (0.031)	0.392	4.989	0.152 (0.030)	0.394	4.911	0.106(0.099)	0.182	2.390

formation of a TM@X_{12} icosahedron around a single $3d$ atom is easier than the production of the X_{13} icosahedral clusters (see also Ref. 35).

The calculated spin and orbital magnetic moments are disclosed in Table II for individual atoms of the TM@X_{12} icosahedra. First, we focus on the induced spin magnetism in the clusters. In the scalar relativistic level, surprisingly the calculated total magnetic moments of all doped clusters are represented by integer values (see Table II). In order to explain this promising feature we concentrate on the related electronic configurations originated from the HOMO levels. The origin of the integer numeral regime for the total spin magnetic moment of TM@X_{12} icosahedra can be understood based on the degeneracy and electron occupation of HOMO levels and symmetry as well as spin polarization of one level below the HOMO levels. These levels are so-called B-HOMO and are listed in Table I. It is found that for those HOMO levels with $h_g(-)$ characters the B-HOMO levels have $h_g(+)$ characters with electron occupation number equal to five. These features cannot be seen for those HOMO levels with $h_g(+)$ (see, for example, the B-HOMO levels of Cu@Au_{12} and Au_{13} clusters in Table I). Therefore one can speculate that those HOMO levels with $h_g(+)$ character are less than half-filled molecular orbitals and those HOMO levels with $h_g(-)$ character are more than half-filled molecular orbitals. According to the above arguments, the total spin magnetic moments of TM@X_{12}, can be obtained as

$$\frac{M_s^T}{\mu_B} = \begin{cases} 5 - n_h & \text{for HOMO } h_g(-) \\ n_h & \text{for HOMO } h_g(+) \end{cases}, \qquad (1)$$

which is based on the first Hund's rule in a superatomic model and the nature of quintuply degenerate h_g representations. The above expression is also in agreement with the 18-electron rule for those clusters with a completely closed shell. As an example, since the individual atoms in the Cr@X_{12} icosahedron have a total of 18 valence electrons we expect that the Cr@X_{12} cluster is a nonmagnetic packing unit. The above expression also results in a vanished total spin magnetic moment for a Cr@X_{12} icosahedron. Our presented DFT calculations for total magnetic moment of all TM@X_{12} icosahedra in the SR level are completely in agreement with the superatomic model (see Table II). We have also calculated the magnetic properties of neutral X_{13} icosahedra with the same noble metal at the center of the clusters (not shown in Table II). In the SR level the calculated GGA total magnetic moments are found at $5\mu_B$ for all three X_{13} clusters which are in agreement

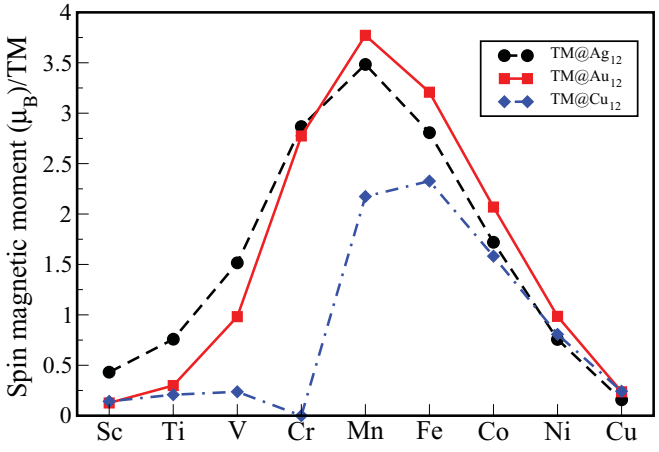

FIG. 4. (Color online) Calculated spin contributions to the magnetic moments of 3*d* TM atoms doped in Cu_{12} (diamond points), Ag_{12} (circle points), and Au_{12} (square points) clusters. The presented data indicate the scalar relativistic calculations.

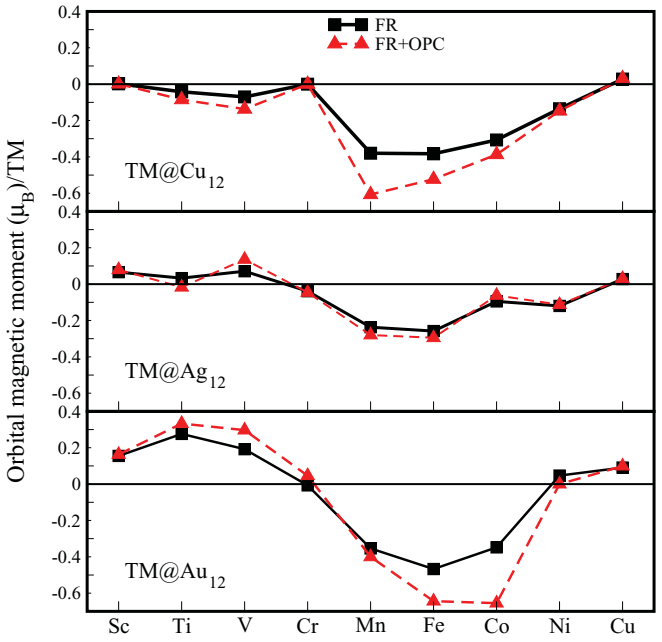

FIG. 5. (Color online) Calculated orbital contributions to the magnetic moments of 3*d* impurities doped in Cu_{12} (top panel), Ag_{12} (middle panel), and Au_{12} (bottom panel) cages. The presented data indicate the orbital moments in the fully relativistic calculations (black square points) and in the presence of OP correction (red triangle points).

with the results based on our superatomic model [$n_h = 5$ and $h_g(+)$ for their HOMO levels]. Other earlier calculations have also reported a total magnetic moment of $5\mu_B$ for a Au_{13} icosahedron.[35,57] However, the reported values of $0.36\mu_B$ for Cu_{13} and $0.28\mu_B$ for Ag_{13} done by Sun and co-workers[33,34] are strongly quenched compared to our findings. Thus, we can argue that the X_{13} clusters behave like the half-filled 3*d* shells in the Mn free atom while the Cr@X_{12} icosahedra are compatible with the Cu free atom with a completely 3*d* closed shell.

The local spin magnetic moments for individual 3*d* atoms doped in the X_{12} icosahedra are shown in Fig. 4. It can be seen that the behavior of spin moments of TM atoms in Ag_{12} and Au_{12} clusters fairly follow the first Hund's rule. However, our results imply that the highest multiplicity principle in a 3*d* single atom doped in Cu_{12} icosahedral cluster is not fulfilled. The origin of these behaviors are also explained in Refs. 33–35. It is worth noting that our findings pronounce that the behavior of local spin magnetism for individual atoms is completely different from the behavior of the total spin magnetic moments of the mentioned icosahedra. It seems that in the SR level calculations, the integer numeral regime for total magnetic moments of the considered clusters may control the individual local spin magnetism through a complex mechanism in a superatomic picture.

In our FR calculations, the total spin magnetic moments are affected by SO interaction marginally with a small deviation from the integer numeral regime. As it is expected, the indirect relativistic effects (more screening of valence electrons from the nuclear charge by inner-shell electrons, see Ref. 40) have a substantial impact on the spin magnetism of the doped Au_{12} icosahedron compared to the Cu_{12} and Ag_{12} clusters. These relativistic effects in gold are strong enough to make more extension and delocalization of its valence 6*s* orbitals. Therefore more hybridization between the 6*s* electrons and 3*d* states of the TM atom causes more aurophilic interactions (metal-metal interactions) and reduces the local spin magnetic moments of the 3*d* atoms. There are noticeable differences between the calculated scalar and fully relativistic spin moments for individual atoms in a gold cluster (see Table II). However, it seems that Ni and Cu atoms in Au_{12} are "abnormal." The total magnetic moments of Ni@Au_{12} and Cu@Au_{12} in a fully relativistic treatment with significant deviations from integer numeral regime are obtained as 0.98 μ_B and 2.44 μ_B, respectively. Even adding an OP correction to the XC functional further reduces the above values. For instance in the presence of OP correction, all valence states in the Ni@Au_{12} cluster, become closed shells and therefore all individual local magnetic moments completely quench (see Table II). It is remarkable to address the question of partially and fully quenched magnetic moments for individual components of the Ni@Au_{12} cluster. One way to suppress the magnetic moments in the Ni@Au_{12} cluster is the effect of more $sp-d$ hybridization due to the extension of 6*s* electrons of gold atoms. More hybridization will cause smaller atomic exchange splitting in Ni atoms between majority and minority 3*d* states. The same scenario can take place for the Cu@Au_{12} cluster. Since Cu@Au_{12} has one electron more than the Ni@Au_{12} icosahedron, rearrangements of the total valence electrons together with strong relativistic effect in peripheral Au atoms cause a total magnetic moment of 2.44 μ_B for Cu@Au_{12} which is larger than the Ni@Au_{12} icosahedra due to its extra electron.

Orbital magnetism is another promising subject in 3*d* atoms doped in the noble clusters. Figure 5 shows the calculated orbital moments of 3*d* atoms doped in X_{12} clusters with and without OP corrections. It can be seen that the 3*d* dopants in Au_{12} have considerably larger orbital moments than in Cu_{12} and Ag_{12}. The orbital moments of Ti and V atoms are very small and negative in the Cu_{12} icosahedron while the orbital moments of these elements gain positive values in Ag_{12} and

Au_{12} icosahedra. The orbital moment of Cr in all three clusters is almost quenched. The orbital moments of Mn, Fe, Co, and Ni doped in X_{12} icosahedra are aligned antiparallel to their spin orientations (except for Ni in Au that its orbital moment is quenched). These trends for the orbital moments of 3*d* elements in X_{12} icosahedra do not significantly change in the presence of OP correction as it can be seen in Fig. 5. These features for orbital magnetism are systematic in all mentioned icosahedral clusters. Our findings are in contradiction to the second Hund's rule in the corresponding 3*d* atoms. In order to understand these discrepancies, we compare our calculated orbital moments to the orbital moments of single 3*d* impurities doped in Cu, Ag, and Au bulk hosts. It is well known that the coinage metals are crystallized in a face centered cubic (FCC) structure and they produce a cubic crystal field. As a consequence of cubic symmetry, the orbital moments of 3*d* impurities are partially quenched. Frota-Pessôa in her relativistic calculations has shown that in the presence of the SO interaction the orbital moments of 3*d* impurities doped in a FCC noble host are very small except for Co that shows a very large orbital moment.[37] It has also been shown that the orbital moments of all 3*d* impurities in FCC structure contain a remnant of second Hund's rule with antiparallel orientations between spin and orbital moments in less than half-filled 3*d* shell and parallel alignments for more than half-filled 3*d* shell.[37] These predictions are confirmed later on by x-ray magnetic circular dichroism (XMCD) measurements for a 3*d* impurity in a Au bulk host.[38] Hence, the symmetry operations in FCC structure preserve the validity of the second Hund's rule for the sign of orbital moments of 3*d* impurities doped in the noble metal hosts. On the other hand, it can be argued that the symmetry operations of an icosahedron with I_h symmetry are the origin of a systematic deviation from the second Hund's rule for the orbital moments of 3*d* atoms doped in the X_{12} clusters (see Fig. 5). The behavior of induced orbital magnetism in TM@X_{12} can be explained based on the superatomic model together with the SO interaction in 3*d* electrons of TM atoms.

It is a well-known fact that the SO coupling causes orbital ordering in TM atoms and because it is rather weak in 3*d* TM atoms (SO coupling parameter $\xi_{SO} \simeq$ 5–100 meV for 3*d* TM series)[54] compare to kinetic and exchange-correlation energies, therefore SO coupling treated as a weak perturbation on the 3*d* TM atoms in SR approach. The size of 3*d* orbital moments can be approximated to first order by the difference of the spin-split 3*d*-resolved partial densities of states (PDOS) at the HOMO level. Figure 6 shows the 3*d*-resolved PDOS for 3*d* TM atoms doped in the Au_{12} icosahedron. Since the 3*d*-resolved PDOS's at the HOMO levels are Lorentzian, based on a simple tight binding model proposed by Ebert and co-workers,[58] we can obtain a very simple expression for the orbital magnetic moments of central TM atoms in the TM@X_{12} icosahedron according to their HOMO level properties:

$$\frac{M_l^{3d}}{\mu_B} \approx \begin{cases} -\xi_{SO} n_{3d}(+,\epsilon_F) & \text{for HOMO } h_g(+) \\ +\xi_{SO} n_{3d}(-,\epsilon_F) & \text{for HOMO } h_g(-) \end{cases}, \qquad (2)$$

where $n_{3d}(+,\epsilon_F)$ and $n_{3d}(-,\epsilon_F)$ are the spin-up and spin-down 3*d*-resolved partial densities of states at the Fermi level. This expression naturally explains the calculated GGA orbital moments in the framework of the FR approach. It can be seen in Fig. 6 that the Cr atom in Au_{12} has a very small minority PDOS at the Fermi level and according to the above expression its orbital moment is almost zero. It can be concluded that for those clusters with completely filled HOMO levels the orbital magnetic moments of 3*d* TM atoms are strongly quenched. Using the above expression, the orbital magnetic moments of $0.05\mu_B$, $0.28\mu_B$, and $0.42\mu_B$, were found for Sc, Ti, and V doped in Au_{12}, respectively. The orbital magnetic moments of $-0.36\mu_B$/Mn, $-0.32\mu_B$/Fe, $-0.48\mu_B$/Co, $-0.57\mu_B$/Ni are calculated. These estimated orbital moments are in qualitative agreement with our DFT calculated orbital magnetic moments for TM@Au_{12} icosahedral clusters (see Table II and Fig. 5). These arguments can be readily extended to explain the orbital magnetic moments of 3*d* atoms doped in Cu_{12} and Ag_{12} icosahedra. Although our superatomic model for orbital magnetic moments is oversimplified due to the assumption of tight binding in the HOMO levels but it can qualitatively explain the deviation of orbital magnetism in doped 3*d* TM atoms from the second Hund's rule. The sign of DFT calculated orbital moments for Ti and V atoms doped in Cu_{12} icosahedra are negative (see Fig. 5) in which they are in contradiction to the prediction of our simple expression based on the superatomic model. As it is mentioned by Sun and co-workers the 3*d* electrons of coppers are strongly hybridized with the 3*d* electrons of the central Ti and V atoms while these hybridizations are marginal for the heavier 3*d* atoms doped in the Cu_{12} icosahedron.[33] These hybridization effects have not been taken into account in our simple model. We can conclude that these hybridization effects reduce and even change the sign of the orbital moments for Ti and V atoms doped in Cu_{12} compared to those calculated orbital moments for Ti and V doped in the Ag_{12} and Au_{12} icosahedra (see Fig. 5). However, we have shown that the second Hund's rule can be preserved in a superatomic picture rather than a single atomic picture. In other words, the total spin (integer numeral regime) and the orbital magnetic moments of 3*d* TM atoms in the icosahedra can be understood when all the valence electrons of the individual atoms rearrange themselves in a superatom.

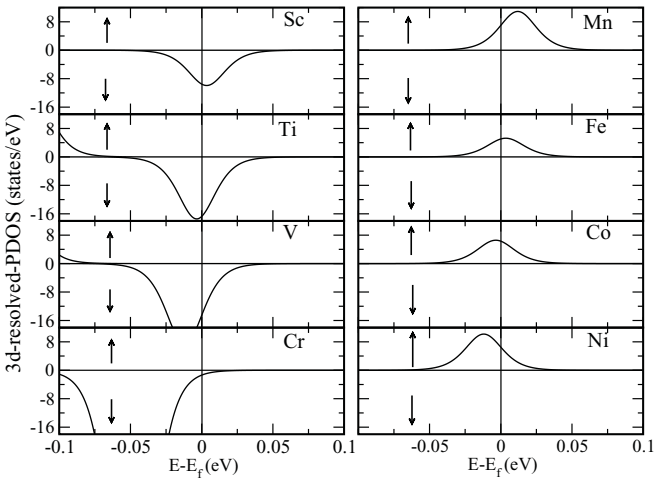

FIG. 6. The 3*d*-resolved partial densities of states in HOMO levels for 3*d* TM atoms doped in icosahedral gold cage. The up (down) arrows indicate the majority (minority) states.

IV. SUMMARY AND CONCLUSIONS

The magnetic properties of a single 3*d* TM atom doped in an icosahedral noble metal cluster were studied using relativistic density functional calculations. We found that the doping of TM atoms would overcome the problem of stabilization at the noble X_{12} icosahedra. The relativistic effects on the magnetic properties of the TM@X_{12} icosahedra were also investigated. Large local magnetic moments have been observed for Mn, Fe, and Co impurities. The self-consistency cycle including fully relativistic effects and OP calculations affect marginally the spin and orbital magnetic moments in Cu and Ag cage icosahedral clusters by a few percent compared to the scalar relativistic self-consistent calculations. We found that the relativistic effects are significant in magnetic properties of the doped gold clusters. On the basis of our magnetic calculations the overriding feature for the TM@X_{12} icosahedral clusters has been the superatomic perspective in order to understand the spin polarization induced in the doped noble metal icosahedron. Relativistic effects together with superatomic picture provide a theoretical framework for rationalizing the orbital magnetism of TM@X_{12} icosahedral clusters. It has to be pointed out that an icosahedron is one of the most symmetric objects between three-dimensional structures. As a consequence we expect that Jahn-Teller distortions may weakly break the symmetry of the icosahedron. For the sake of simplicity the Jahn-Teller distortions are neglected in our calculations. The Jahn-Teller distortions, as well as noncollinear magnetism as second-order corrections, can be taken into account to give rise to more accurate ground states. We suggest further experiments such as XMCD measurements to check our predictions on spin and orbital magnetism of the TM@X_{12} icosahedra.

ACKNOWLEDGMENTS

We are grateful to Manuel Richter for valuable discussions. The computing facilities of High Performance Computational Laboratory at Department of Physics, Iran University of Science and Technology (IUST) were used. Financial support by research division at IUST is gratefully acknowledged.

*sargolzaei@iust.ac.ir

[1] P. Schwerdtfeger, Angew. Chem. Int. Ed. **42**, 1892 (2003).
[2] N. Agraït, A. L. Yeyati, and J. M. van Ruitenbeeck, Phys. Rep. **377**, 81 (2003).
[3] M. C. Daniel and D. Astru, Chem. Rev. **104**, 293 (2004).
[4] P. Pyykkö, Angew. Chem. Int. Ed. **43**, 4412 (2004).
[5] D. L. Lu and K. I. Tanaka, Phys. Rev. B **55**, R13865 (1997).
[6] S. Ogawa and S. Ino, J. Cryst. Growth **13**, 48 (1972).
[7] D. G. Leopold, J. Ho, and W. C. Lineberger, J. Chem. Phys. **86**, 1715 (1987).
[8] S. Bulusu, X. Li, L. S. Wang, and X. C. Zeng, PNAS **103**, 8326 (2006).
[9] X. Xing, B. Yoon, U. Landman, and J. H. Parks, Phys. Rev. B **74**, 165423 (2006).
[10] H. Häkkinen, M. Moseler, and U. Landman, Phys. Rev. Lett. **89**, 033401 (2002).
[11] W. Fa, C. Luo, and J. Dong, Phys. Rev. B **72**, 205428 (2005).
[12] X. Gu, M. Ji, S. H. Wei, and X. G. Gong, Phys. Rev. B **70**, 205401 (2004).
[13] R. Arratia-Pérez, A. F. Ramos, and G. L. Malli, Phys. Rev. B **39**, 3005 (1989).
[14] Q. Sun, Q. Wang, P. Jena, and Y. Kawazoe, ACS Nano **2**, 341 (2008).
[15] D. Tian and J. Zhao, J. Phys. Chem. A **112**, 3141 (2008).
[16] E. M. Fernández, J. M. Soler, I. L. Garzón, and L. C. Balbás, Phys. Rev. B **70**, 165403 (2004).
[17] E. Janssens, H. Tanaka, S. Neukermans, R. E. Silverans, and P. Lievens, Phys. Rev. B **69**, 085402 (2004).
[18] Y. Dong and M. Springborg, Eur. Phys. J. D **43**, 15 (2007).
[19] L. D. Marks and D. J. Smith, J. Cryst. Growth **54**, 425 (1981).
[20] B. A. Collings, K. Athanassenas, D. Lacombe, D. M. Rayner, and P. A. Hackett, J. Chem. Phys. **101**, 3506 (1994).
[21] K. J. Taylor, C. L. Pettiette-Hall, O. Cheshnovsky, and R. E. Smalley, J. Chem. Phys. **96**, 3319 (1992).
[22] H. Häkkinen, B. Yoon, U. Landman, X. Li, H. J. Zhai, and L. S. Wang, J. Phys. Chem. A **107**, 6168 (2003).
[23] M. P. Johansson, A. Lechtken, D. Schooss, M. M. Kappes, and F. Furche, Phys. Rev. A **77**, 053202 (2008).
[24] E. Janssens, S. Neukermans, H. M. T. Nguyen, M. T. Nguyen, and P. Lievens, Phys. Rev. Lett. **94**, 113401 (2005).
[25] E. F. Kustov and V. I. Nefedov, Dokl. Phys. Chem. **409**(1), 188 (2006).
[26] G. Zanti and D. Peeters, J. Phys. Chem. A **114**, 10345 (2010).
[27] P. Pyykkö, and N. Runeberg, Angew. Chem. int. Ed. **41**, 2174 (2002).
[28] X. Li, B. Kiran, J. Li, H.-J. Zhai, and L.-S. Wang, Angew. Chem. Int. Ed. **41**, 4786 (2002).
[29] H. J. Zhai, J. Li, and L. S. Wang, J. Chem. Phys. **121**, 8369 (2004).
[30] S. Neukermans, E. Janssens, H. Tanaka, R. E. Silverans, and P. Lievens, Phys. Rev. Lett. **90**, 033401 (2003).
[31] Y. X. Qiu, S. G. Wang, and W. H. E. Schwarz, Chem. Phys. Lett. **397**, 374 (2004).
[32] M. X. Chen and X. H. Yan, J. Chem. Phys. **128**, 174305 (2008).
[33] Q. Sun, X. G. Gong, Q. Q. Zheng, D. Y. Sun, and G. H. Wang, Phys. Rev. B **54**, 10896 (1996).
[34] Q. Sun, Q. Wang, J. Z. Yu, Z. Q. Li, J. T. Wang, and Y. Kawazoe, J. Phys. I **7**, 1233 (1997).
[35] Sh.Y. Wang, J. Z. Yu, H. Mizuseki, Q. Sun, C. Y. Wang, and Y. Kawazoe, Phys. Rev. B **70**, 165413 (2004).
[36] N. Papanikolaou, N. Stefanou, R. Zeller, and P. H. Dederichs, Phys. Rev. B **46**, 10858 (1992).
[37] S. Frota-Pessôa, Phys. Rev. B **69**, 104401 (2004).
[38] W. D. Brewer, A. Scherz, C. Sorg, H. Wende, K. Baberschke, P. Bencok, and S. Frota-Pessôa, Phys. Rev. Lett. **93**, 077205 (2004).
[39] M. Sargolzaei, I. Opahle, M. Richter, K. Koepernik, U. Nitzsche, and H. Eschrig, J. Magn. Magn. Mater. **290-291**, 364 (2005).
[40] P. Pyykkö, Angew. Chem. **114**, 3723 (2002).
[41] D. J. Gorin and F. D. Toste, Nature (London) **446**, 395 (2007).

[42]P. Schwerdtfeger, Heteroatom Chemistry **13**, 578 (2002).
[43]I. Opahle, Ph.D. thesis, TU Dresden, 2001; H. Eschrig, M. Richter, and I. Opahle, in *Relativistic Electronic Structure Theory - Part II: Applications*, edited by P. Schwerdtfeger (Elsevier, Amsterdam, 2004), pp. 723–776.
[44]A. Yang, W. Fa, and J. Dong, J. Phys. Chem. A **114**, 4031 (2010).
[45]D. E. Jiang and R. L. Whetten, Phys. Rev. B **80**, 115402 (2009).
[46]X. Li, B. Kiran, L. F. Cui, and L. S. Wang, Phys. Rev. Lett. **95**, 253401 (2005).
[47]J. Botana, M. Pereiro, D. Baldomir, J. E. Arias, K. Warda, and L. Wojtczak, J. Appl. Phys. **103**, 07B716 (2008).
[48]P. Hohenberg and W. Kohn, Phys. Rev. **136**, B864 (1964).
[49]FPLO-9.00-33 [improved version of the original FPLO. code by K. Koepernik and H. Eschrig, Phys. Rev. B **59**, 1743 (1999)]; [http://www.FPLO.de].
[50]J. P. Perdew, K. Burke, and M. Ernzerhof, Phys. Rev. Lett. **77**, 3865 (1996).
[51]O. Eriksson, M. S. S. Brooks, and B. Johansson, Phys. Rev. B **41**, 7311 (1990).
[52]H. Eschrig, M. Sargolzaei, K. Koepernik, and M. Richter, Europhys. Lett. **72**, 611 (2005).
[53]M. Sargolzaei, *Orbital Polarization in Relativistic Density Functional Theory* (Lambert Academic Publishing, Saarbrücken, Germany, 2010).
[54]M. Richter, "Density Functional Theory applied to 4f and 5f Elements and Metallic Compounds," in *Handbook of Magnetic Materials* edited K. H. J. Buschow (Elsevier, Amsterdam, 2001), Vol. 13.
[55]M. D. Morse, Chem. Rev. (Washington, D. C.) **86**, 1049 (1986).
[56]B. Simard and P. A. Hackett, J. Mol. Spectrosc. **142**, 310 (1990).
[57]W. Luo, S. J. Pennycook, and S. T. Pantelides, Nano Lett. **7**, 3134 (2007).
[58]H. Ebert, R. Zeller, B. Drittler, and P. H. Dederichs, J. Appl. Phys. **67**, 4576 (1990).